Arch. Metall. Mater., Vol. 61 (2016), No 4, p. 1945–1952

DOI: 10.1515/amm-2016-0313

M. WINNICKI*,#, M. RUTKOWSKA-GORCZYCA*, A. MAŁACHOWSKA*, T. PIWOWARCZYK*, A. AMBROZIAK*

MICROSTRUCTURE AND CORROSION RESISTANCE OF ALUMINIUM AND COPPER COMPOSITE COATINGS DEPOSITED BY LPCS METHOD

The paper presents the study of microstructure and corrosion resistance of composite coatings ($Al+Al_2O_3$ and $Cu+Al_2O_3$) deposited by Low Pressure Cold Spraying method (LPCS). The atmospheric corrosion resistance was examined by subjecting the samples to cyclic salt spray and Kesternich test chambers, with NaCl and SO_2 atmospheres, respectively. The selected tests allowed reflecting the actual working conditions of the coatings. The analysis showed very satisfactory results for copper coatings. After eighteen cycles, with a total time of 432 hours, the samples show little signs of corrosion. Due to their greater susceptibility to chloride ions, aluminium coatings have significant corrosion losses.

Keywords: cold spraying, composite coatings, cyclic salt spray test, Kesternich test

1. Introduction

The method of gas dynamic cold spraying is one of the latest methods of thermal spraying. It was invented in the 1980s in the Soviet Union, and due to the numerous advantages undergoes constant development to this day. The innovation of this method relies on the way to build the coating. The metal powder used for spraying does not melt in the gas stream. The powder particles strike the substrate in the solid state, making the coating structure uniform. This translates to very good mechanical, physical and chemical properties of the deposited coatings [1-9]. In the cold spraying method, powder particles acquire velocity from the compressed stream of heated gas (air, nitrogen or helium). The final properties of the coating are determined by the same process parameters as in other thermal spray processes, i.e. the velocity and temperature of the particles [1,2,6-8]. The kinetic energy required to deposit the particles on the substrate is provided by the supersonic velocity of particles, obtained in the process.

The bonding between the substrate material and the powder particles occurs if the so-called critical velocity is exceeded[1-5]. One can distinguish two varieties of the cold spray method: low-pressure cold spraying method (LPCS) and high-pressure cold spraying method (HPCS). In the LPCS method, nitrogen or air at a pressure and temperature up to 1 MPa and 700 °C, respectively, is used as the working gas. It is intended primarily for spraying soft metal, such as Sn, Zn, Al, Cu, Ni, and Fe. A key factor in increasing the corrosion resistance of the coating is to reduce its porosity. By lowering the porosity an increase in the density of the coating is obtained, which can be achieved by adding a ceramic phase to the powder [3,10-17]. The most preferred properties of the copper composite coating were observed at 50% vol. addition of Al_2O_3 [13].

Aluminium is a material often used in the cold spray method, due to its low weight and high toughness [18]. Coatings deposited using this method show a high resistance to corrosion, similar to pure aluminium, and hardness higher than that of cold rolled aluminium sheets [19].

Aluminium corrodes in slightly and highly acidic or slightly and highly alkaline atmospheres. An insoluble corrosion products of aluminium are stable in neutral reaction and oxidizing conditions, thus aluminium passivation is recommended [20,21]. To protect aluminium against corrosion dense anodic coatings with more noble material should be deposited [20].

Copper is a material often used to build coatings by cold spraying due to its high electrical conductivity and corrosion resistance properties. Moreover copper shows high corrosion resistance due to copper oxide that stabilize the copper surface by creating thin layer of patina [22]. Cold sprayed copper coatings shows high stability also in anaerobic environment and can be applied in chambers for worn out radioactive wastes [23].

There is a lot of methods concerning the analysis of materials corrosion protection [24-27]. The corrosion tests under controlled conditions of humidity and cyclic salt spray show a very good correlation with the actual operating conditions in which there is a large influence of chloride ions [24,25].

The corrosion tests under controlled conditions of humidity and cyclic salt spray are used to assess the corrosion resistance of metals in environments in which there is a large influence of chloride ions. Although there is no direct correlation between metals resistance to corrosion in salt fog and resistance to corrosion in natural environment due to presence of other media, the test provides valuable comparative information about performance in conditions similar to those used in the test [26,27]. Therefore salt spray test is a main test used in automobile industry to control materials quality [26].

* WROCŁAW UNIVERSITY OF TECHNOLOGY, 5 ŁUKASIEWICZA STR., 50-371, WROCŁAW, POLANDABSTRACT

** Corresponding author: marcin.winnicki@pwr.edu.pl

Whereas in order to simulate industrial and urban atmospheres a test with a general condensation of moisture and sulfur dioxide is used, which is known as the Kesternich test [28]. Kesternich test is used i.e. to assess the resistance of coated steel sheets to atmospheric corrosion and acid rain or in electronics industry [28-30]. The test consists in the formation of an artificial atmosphere containing SO_2 and optionally CO_2.

However, there is very limited data concerning the corrosion resistance of coatings working as an interlayer in the Al-Cu current contacts. Such contacts often appear in electric connectors, e.g. busbars, and in order to secure materials form corrosion, one or both of the contact interfaces must be coated. Particularly little information on this topic regards coatings deposited by low-pressure cold spraying. Hence, in this article natural conditions were simulated, carrying out tests in the salt chamber and the Kesternich test. The microstructure and corrosion resistance of aluminium and copper coatings, deposited onto the copper and an aluminium alloy substrates, respectively, were examined.

2. Research methodology

The coatings were sprayed using the DYMET 413 and air as the working gas. Spraying parameters are listed in tab. 1. Two commercially available powders: spherical Al (K-10-01) with a particle size of -45+10 µm and 60% wt. Al2O3 addition (fig. 1a) and dendritic Cu (K-01-01) with a particle size of -50+10 µm and 50% wt. Al_2O_3 addition (fig. 1b) (Obnisk Centre for Powder Technology, Russia) were used in the study. The ceramics content was given according to the supplier's data sheet. Alumina phase is visible in the picture as the particles with polyhedral shape (Fig. 1).

Morphology, size and distribution of used powder was analysed using a scanning electron microscope (ZEISS EVO 25 MA, Jena, Germany) and a particle size analyzer (Partica LA-950V2 , Tokyo, Japan).

The substrate material were plates with dimensions 7x25x100 mm made of pure copper M1E and aluminium alloy AW 1350 with the following chemical composition (as per PN-EN 573-3:2010P, % weight): 0.1% Si (max.), 0.4% Fe (max.), 0.05% Cu (max.), 0.01% Cr (max.), 0.05% Zn (max.), 0.1% others (max.) and 99.5% Al. (min.). The aluminium powder was deposited onto a copper substrate, and the copper powder on the aluminium substrate. Prior to spraying, the substrate surface has been subjected to sand-blasting with alumina, particle size of 800 µm.

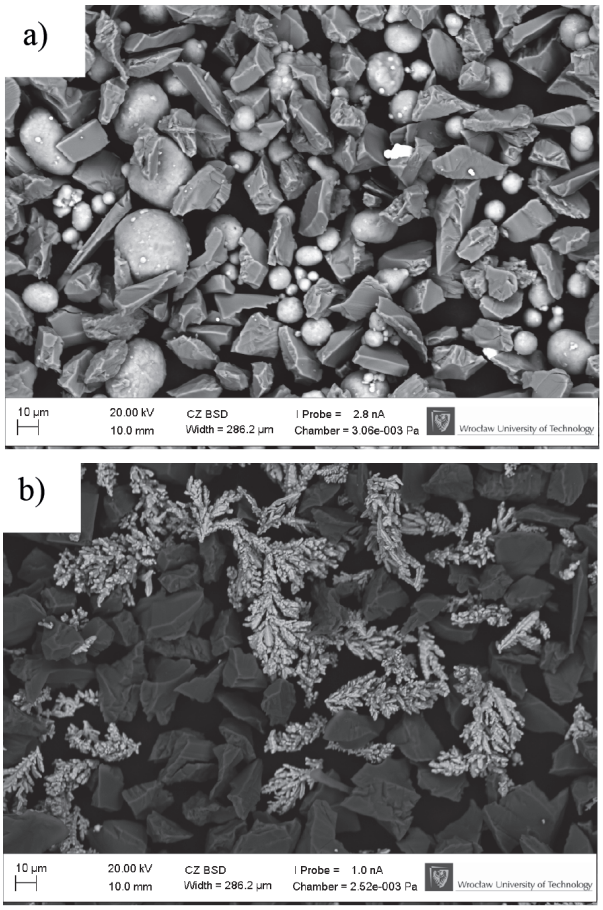

Fig. 1. Morphology of powders used in LPCS: Al+Al_2O_3 (a) and Cu+Al_2O_3 (b)

The microstructure of the coatings was analysed using a scanning electron microscope Phenom G2 pro. Before the tests, metallographic aluminium and copper samples were etched according to PN-75/H-04512 for 1 minute in the room temperature in 10% aqueous solution of hydrofluoric acid and 10% aqueous solution of ammonium persulfate, respectively. Samples of the corrosion tests were analysed using a light microscope Nikon Eclipse MA 200 and the NIS Elements BR program. Metallographic cross-sections were prepared by cutting the sample 15 mm from the bottom edge. The chemical composition of the coating surfaces after the corrosion tests was analysed using SEM ProX Phenom. The analysis was performed at five different points at a distance of 30 mm from the lower edge of the sample.

TABLE 1

LPCS process parameters

Powder	Thickness of the coating after machining h [µm]	Number of layers in the coating	Input parameters					
			Powder feeding rate mp [g/min]	Linear velocity υl [mm/s]	Gas pressure pg [MPa]	Gas temperature Tg [°C]	Stand-off distance l [mm]	Distance between two adjacent beads l [mm]
Al+Al_2O_3	300	1	40	10	0.9	600	10	3.5
Cu+Al_2O_3								

Before the coating corrosion test, the samples were machined. Then the roughness and waviness of the machined surface was determined using profilographometer Form Talysurf 120L.

The corrosion resistance test in a salt chamber with cyclical salt spray was carried out in accordance with PN-EN ISO 16701-2010P. In the first, wet cycle of the test, the samples were subjected to continuous spraying with an aqueous 5% NaCl solution acidified to pH 4.2 at 35 °C. In the next cycle, the samples were exposed to the atmosphere with a humidity of between 95% RH and 50% RH at a constant temperature of 35 °C. Both cycles lasted 12 hours and were performed alternately. In performed research, after completing a single cycle, the samples were placed at ambient conditions of average temperature of 22 °C and humidity of 55% RH for the next 12 hours.

The examinations using the Kesternich test were performed in accordance with PN-EN ISO 6988-2000P. In the first cycle, which lasted 8 hours, the samples were closed in a climate chamber with a capacity of 300 l, which was fed with 2 l of SO2 at humidity of 100% RH and temperature of 40 °C. In the second cycle, lasting 16 hours, the chamber was open and the samples were exposed to ambient temperature of 22 °C. In both tests 18 cycles were performed, with a total examination time of 432 hours.

3. Results and discussion

After spraying Al+Al_2O_3 coatings had a thickness in the range of 410-650 µm and were machined to 300 µm. The coating structure is composed of three areas: aluminium

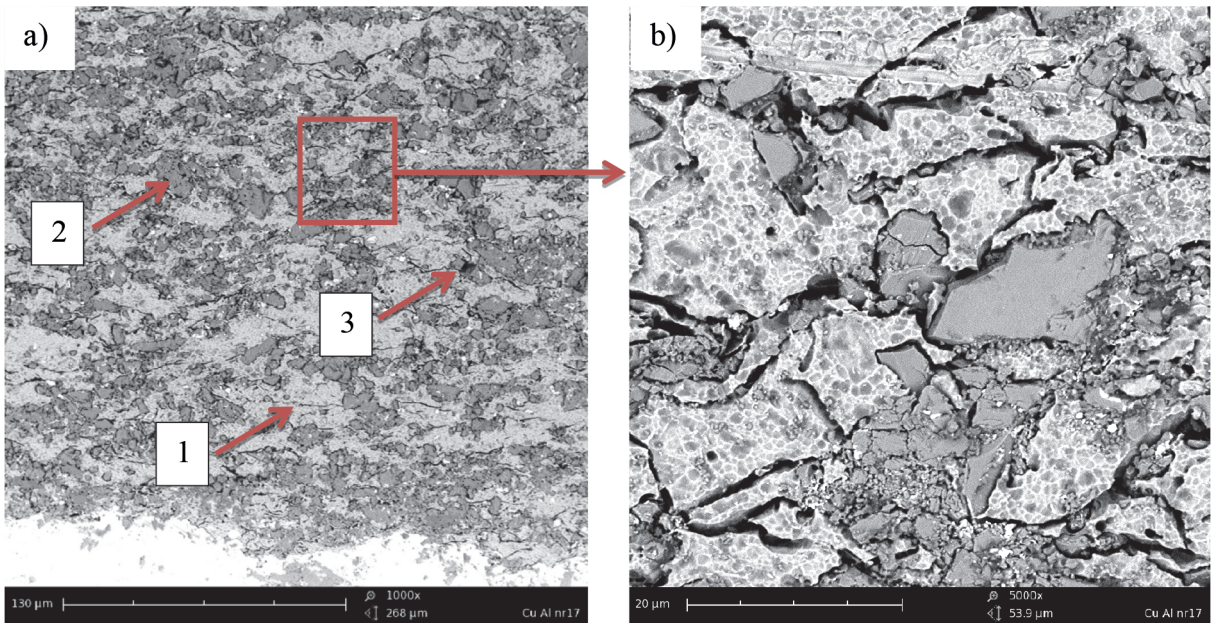

Fig. 2. Microstructure (SEM) of the coating Al+Al_2O_3 (a,b), etched with 10% solution of sodium hydroxide

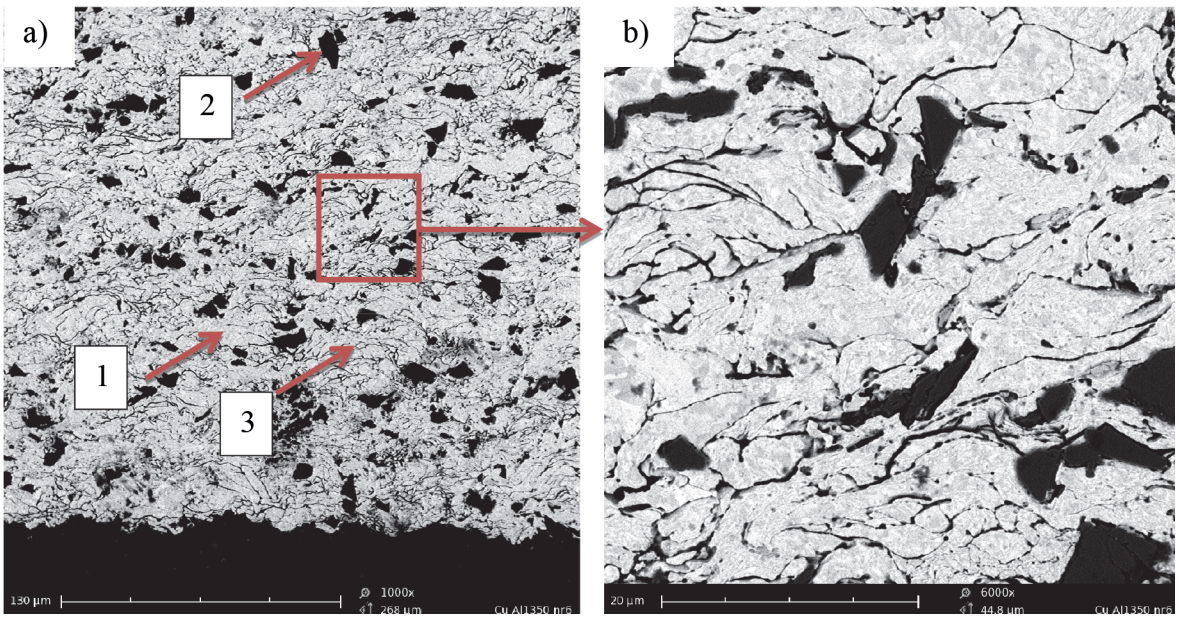

Fig. 3. Microstructure (SEM) of the coating Cu+Al_2O_3 (a,b), etched with 10% solution of ammonium persulfate

particles (1), alumina (2) and pores (3) (Fig. 2). Despite the use of high temperatures of 600 ˚C in the process, the coating did not show oxidation. The presence of alumina, which tamps the metal, provides high density and minimizes the presence of pores [13,16,31].

Coatings deposited with Cu+Al_2O_3 powder had a thickness in the range 330-560 µm after spraying and before corrosion tests were machined to 300 µm thickness (Fig. 3). The oxidation of metal particles is also invisible. The fine particles of alumina are deposited in large amounts between the individual copper particles to form a local reinforcement. The porosity is lower than in the case of aluminium coatings. Pores are present only on the particles boundaries. On the one hand aluminium has higher critical velocity than copper [7]. On the other hand copper powder morphology contributed significantly to the deposition behaviour [32]. Irregular particles are accelerated to higher velocities and upon the impact deform easier which is assigned to inter-particle friction and hence particle temperature rises [33]. This results in lower porosity especially when ratio of particle velocity to critical one is low. However as reported by Koivuluoto et. al [13] the microporosity is present in coatings deposited of dendritic copper powder and thus spherical copper powder exhibit better results in open-cell potential measurements. Despite the similar volume ratio of alumina in powder, the microstructure image shows that much more alumina is deposited in aluminium coatings, which is in an amount of 30-34% vol., while the in the copper coating it is about 6-8% vol.

Apart from the large Al_2O_3 particles at the border aluminium particles, there are intensive agglomerations of fine Al_2O_3 within single Al particles (Fig. 4). The presence of fine Al_2O_3 particles with size in the range from about 500 nm to 3 µm result from collision of ceramic particles with each other. The Al_2O_3 particles cannot deform and after collision are partially fragmented and rebounded. The high initial concentration of ceramics increases the intensity of this phenomenon [13,16].

The higher ceramics content in the aluminum coatings than in copper ones might be prescribed to the difference in material properties. The ceramic particles cannot form metallic bonding after hitting the substrate, thus they just stick to the metal matrix and interlock with metal particles [13]. These phenomena are favourable for aluminum powder which has lower mechanical properties and hence is easier to penetrate by ceramic particles. Additionally lower softening temperature of aluminum causes that it is “more sticky” in elevated temperature and the fragmented Al_2O_3 particles bond easier. It might be seen that in case of copper characterized by higher melting temperature and mechanical properties very few fragmented Al_2O_3 particles are present (Fig. 4).

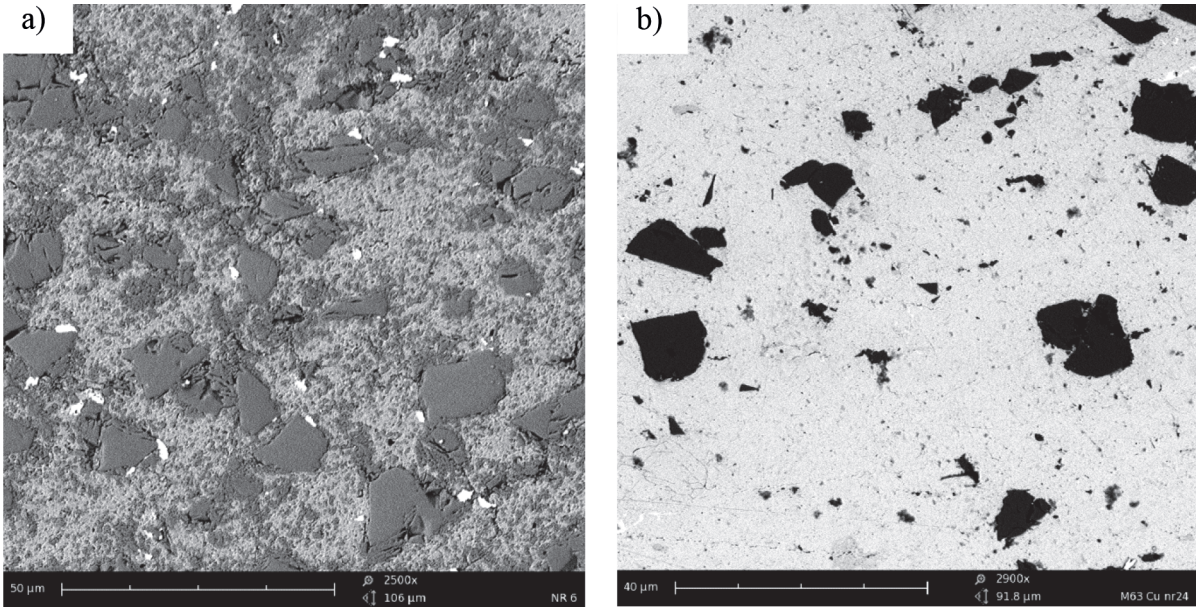

Fig. 4. Comparison of the content of fine alumina particles in aluminium (a) and copper (b) coatings, sample unetched

TABLE 2

Measurement results of the coatings surface roughness and waviness

Coating	Roughness, µm				Waviness, µm			
	Ra	σ	*Rt*	σ	*Wa*	σ	*Wt*	σ
Cu-Al_2O_3	0.50	0.13	12.2	0.20	9.1	3.95	42.0	15.29
Al-Al_2O_3	0.62	0.09	16.01	4.45	19.3	4.94	84.26	19.21

σ – standard deviation

Stereometric measurements results of the coatings surface are shown in Tab. 2. Surface roughness and waviness plays an important role in corrosion resistance of metals. It has been reported that polished surface of stainless steel exhibit lower susceptibility to pitting corrosion and overall lower corrosion rates [34,35]. This effect was also observed for cold sprayed titanium coatings [36]. Therefore the sprayed coatings were machined and the surface roughness and waviness are given as a reference data.

A view of the samples coated with $Al+Al_2O_3$ and $Cu+Al_2O_3$ prior to corrosion testing as well as after 1 and 18 cycles in the chamber with NaCl and SO_2 atmospheres are shown in Fig. 5 and 6, respectively. Corrosion tests of aluminium coatings in the climate chamber with NaCl showed significant corrosion changes. The protective oxide layer present on the aluminium surface has already been locally dissolved after one cycle (Fig. 5b), as aluminium exhibits poor resistance to acids and bases. The film is particularly vulnerable to destruction in the presence of chlorides [37,38]. As a result of the Cl- environment, white spots were observed, which increased considerably after the last cycle (Fig. 5c). These are complex corrosion compounds of aluminium, based on chlorohydrates.

In the case of Cu coatings, after one cycle (Fig. 6b) green areas of patina deposit on the surface appeared. After another 17 cycles the deposits grew (Fig. 6c), turning into the black areas, giving evidence of local surface corrosion. In the marine environment, simulated by the test with the use of sodium chloride, the predominantly formed deposits include cuprite Cu_2O, malachite $CuCO_3 \cdot Cu(OH)_2$, copper hydroxychloride $Cu_7Cl_4(OH)10 \cdot H_2O$,the less common nantokite CuCl and eriochalcite $CuCl_2 \cdot 2H_2O$ [23].

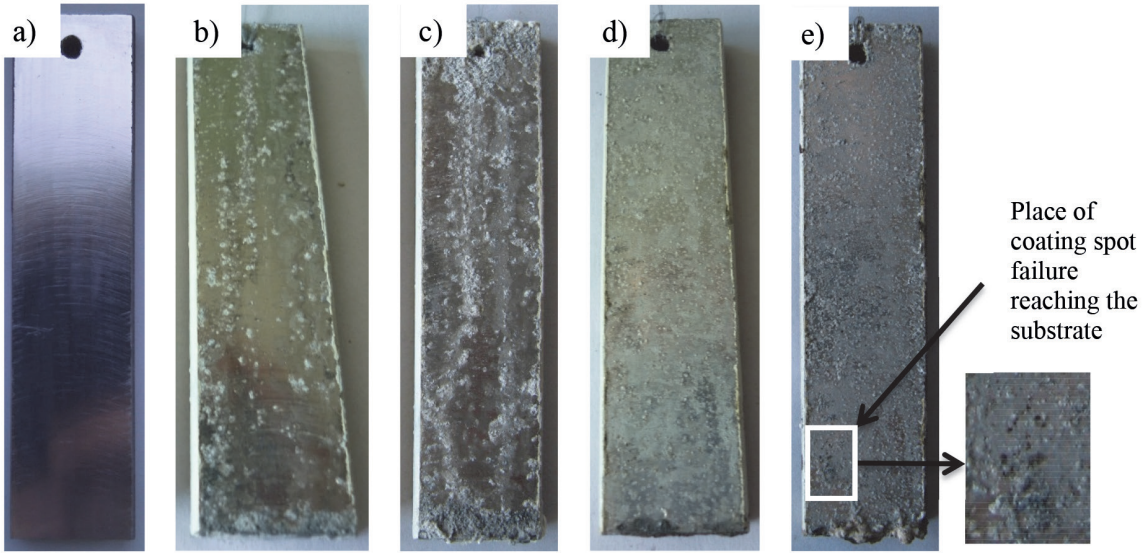

Fig. 5. Samples with $Al+Al_2O_3$ coatings deposited by LPCS, after machining (a), after one cycle (b) and 18 cycles (c) in the NaCl chamber, after one cycle (d) and 18 cycles in the SO2 chamber (e)

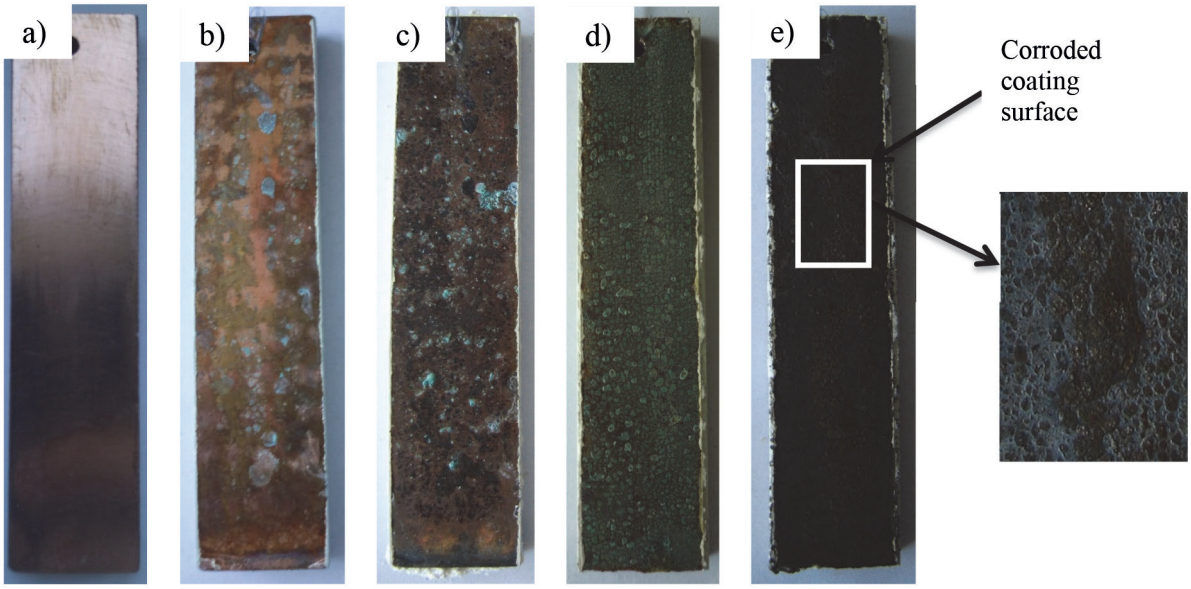

Fig. 6. Samples with $Cu+Al_2O_3$ coatings deposited by LPCS, after machining (a), after one cycle (b) and 18 cycles (c) in the NaCl chamber, after one cycle (d) and 18 cycles in the SO2 chamber (e)

The corrosion test in a climate chamber with SO_2 after 1 cycle showed significant surface changes of both, $Al+Al_2O_3$ and $Cu+Al_2O_3$ coatings (Fig. 5d and 6d). Both samples were covered with corrosion products visible as a green patina for copper and white layer for aluminium. In the case of $Al+Al_2O_3$ coatings, spot discoloration is also visible as evidence of corrosion of aluminium. Already after 5 cycles, the sample showed clear macroscopic Al corrosion manifestations due to the local dissolution of the coating. After 18 cycles, the amount of corrosion increased and reached the depth of the substrate (Fig. 5e). In the case of $Cu+Al_2O_3$ coatings, the upper part was covered with a single layer of black patina (Fig. 6e). It was composed of water insoluble compounds, such as cuprite Cu_2O, antlerite $Cu_3(OH)_4SO_4$ and posnjakite $Cu_4(OH)_6SO_4 \cdot H_2O$ [38]. Furthermore, while in the SO_2 atmosphere, the patina may additionally contain other hydroxy-sulphates [39].

Samples sprayed before corrosion testing were secured on the long edges with paint. Shorter edges remained unprotected. After the corrosion test of $Al+Al_2O_3$ coatings in

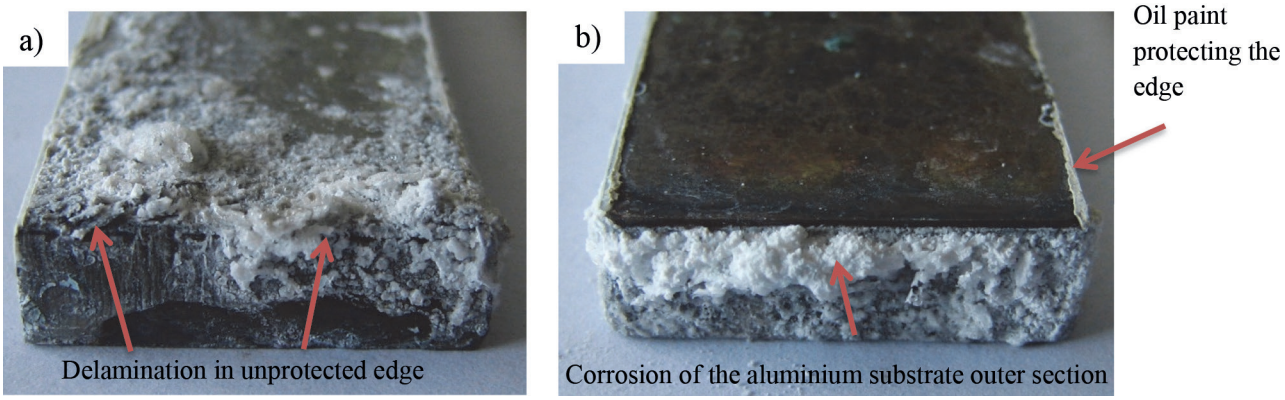

Fig. 7. Corrosion on the edges of the sample after the salt spray test, $Al+Al_2O_3$ (a) and $Cu+Al_2O_3$ (b) coatings

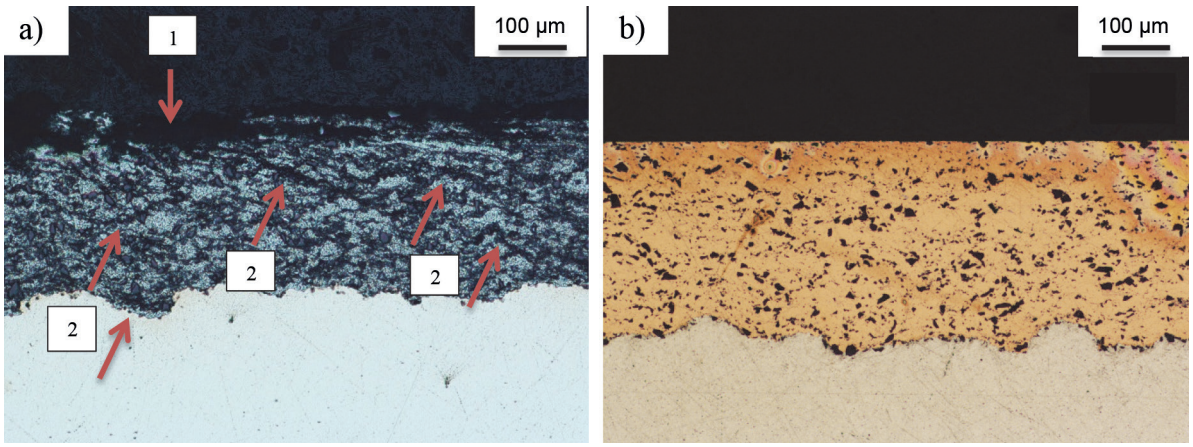

Fig. 8. The microstructure of the $Al+Al_2O_3$ (a) and $Cu+Al_2O_3$ (b) coatings with corrosive changes after the test in a chamber with NaCl. 1 - dissolved surface of the coating, 2 - a crack in the coating caused by stress corrosion

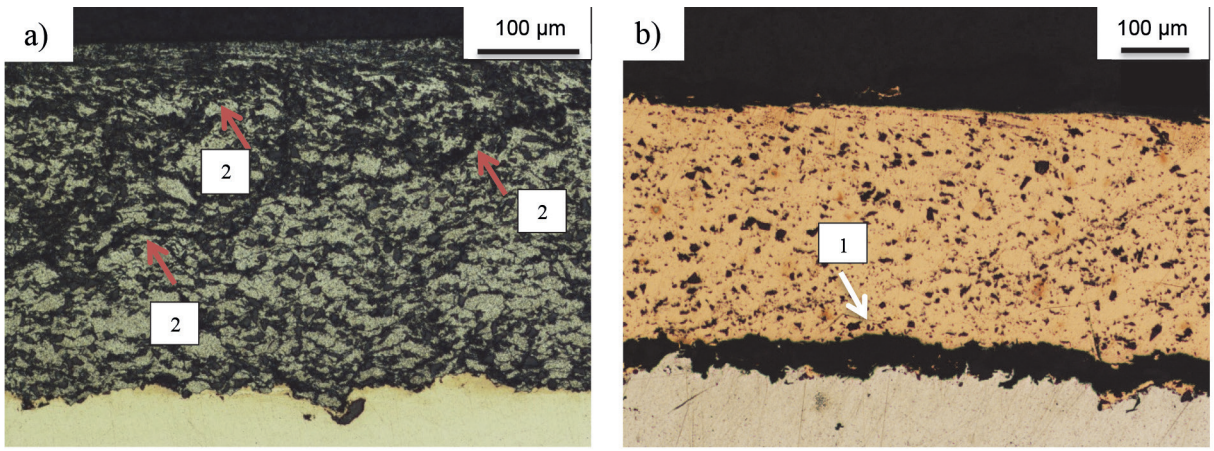

Fig. 9. The microstructure of the $Cu+Al_2O_3$ (a) and $Al+Al_2O_3$ (b) coatings after the test in a chamber with SO_2. 1 - delamination caused by galvanic corrosion, 2 - a crack in the coatings caused by stress corrosion

TABLE 3

Analysis of the chemical composition of the coatings after the corrosion test

Coating	Corrosion atmosphere	Chemical composition of coating surface [mean wt. %]					
		Al	O	Cu	Cl	Na	S
Al+Al_2O_3 on Cu	NaCl	54.8	43.2	0.3	0.2	1.5	0.0
Al+Al_2O_3 on Cu	SO2	38.6	57.9	0.3	0.0	0.0	3.2
Cu+Al_2O_3 on AW1350	NaCl	5.5	35.7	49.8	1.3	7.7	0.0
Cu+Al_2O_3 on AW1350	SO2	7.9	55.1	30.1	0.0	0.0	6.9

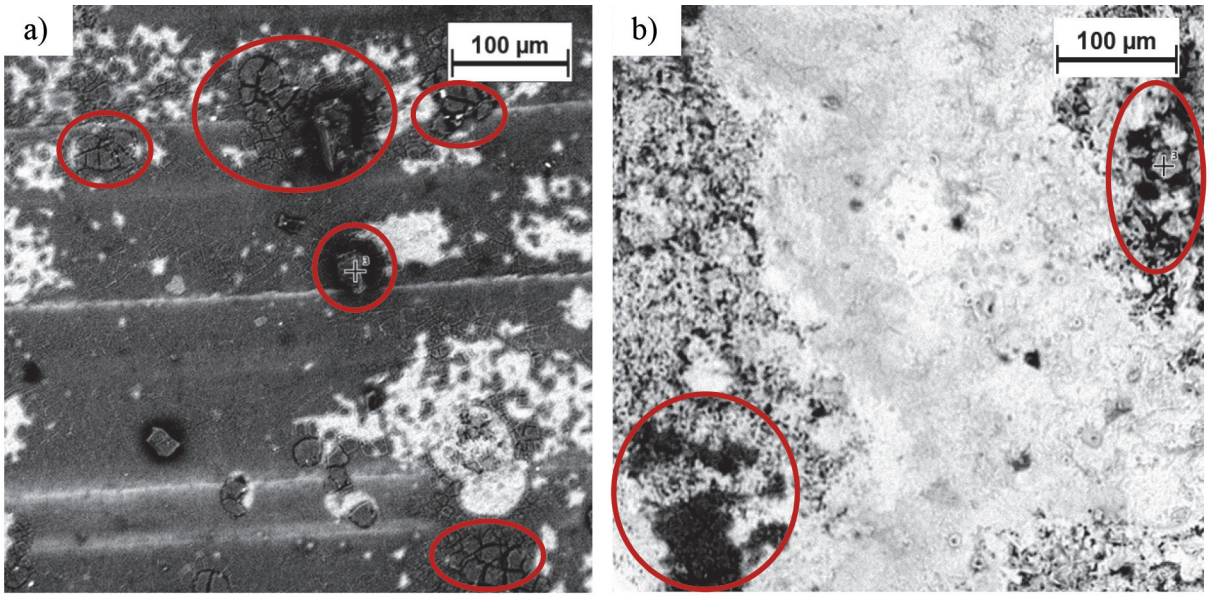

Fig. 10. The most intensively oxidized spots in the Al+Al_2O_3 (a) and Cu+Al_2O_3 (b) coatings after the Kesternich test

a salt chamber, the top layer of the sample was covered by an intense white coating, which is a result of corrosion of aluminium and reflects the dissolution of the coating. One can also notice delamination on the unprotected edge of the sample, which most likely is the result of stress corrosion cracking (Fig. 7a). Thermally sprayed coatings are always accompanied by internal residual stress [1,3,40]. Despite the occurrence of mostly compressive stresses in LPCS method [1] in the contact area between the LPCS coating and the substrate, the presence of Cl- ions in the environment has increased electromotive force of the corrosion cell in this area. This is facilitated by the powder particles work-hardening during spraying [25]. Corrosion has led to the delamination, due to which the crack went deeper into the material, parallel to the longer edges (Fig. 8a). In this case, the aluminium coating acts as the anode, so undergoes corrosion, protecting the copper substrate against corrosion.

Despite the large difference in potential between the Cu coating material and the substrate alloy AW1350, there was no corrosion on the edge of the sample (Fig. 7b). The microstructure of the coatings showed no corrosion changes (Fig. 8b). Being a cathode coating, copper coating hermetically protects the aluminium substrate against corrosion. Both the copper and the aluminium coatings provided satisfactory corrosion resistance, that no corrosion in protected substrate has been noticed.

The aluminium coating after the test in an environment of sulfur oxide, just like the sample after the salt spray test, shows the presence of cracking caused by stress corrosion (Fig. 9a). It has been started by the local pitting corrosion initiated on the surface of the coating. However, no losses in the thickness of the coating were recorded. The passive oxide layer on the aluminium surface is resistant to sulfur environment.

The Cu+Al_2O_3 coating exhibits intense corrosive activity. Corrosion led to delamination of the coating (Fig. 9b), which is most likely caused by galvanic corrosion. The crack also indicates the emergence of corrosion spots in the substrate material which has a lower potential. The crack was observed only in the axis of the sample, hence the conclusion that it advanced from the unprotected edge.

The results of the chemical composition analysis of coatings surface after testing in the two atmospheres are shown in Table 3. For both, aluminium and copper coatings, the testing in SO_2 atmosphere caused higher oxidation, as evidenced by the higher percentage of oxygen and a lower of metal on the surface of the coating. The coatings surface oxidation spots are marked in Fig. 10. In the case of copper-coated samples the presence of Al in the range of 5-8% was noted. However, metallographic examination excluded the probability of dissolution of the coating or pitting corrosion reaching the substrate. Hence it is believed that the presence of aluminium is derived from the upper unprotected edges of the samples, which were characterized by intensive corrosion.

4. Conclusions

In the studies copper and aluminium coatings deposited by LPCS were analysed. Both materials allowed for spraying dense, free of pores and oxidation coatings. It arise from the addition of the ceramic admixture, which work-hardened the metal powder during spraying. The atmospheric corrosion examinations with salt spray and Kesternich tests clearly indicate a greater corrosion resistance of copper coatings. The copper coated sample after testing in a salt solution showed no changes. The Kesternich test led to galvanic corrosion, which began in the unprotected edges and advanced into the material.

Aluminium coatings after the test in the cyclic NaCl spray showed a delamination and a local dissolution of the coating. Additionally, due to stress corrosion, cracking occurred within the coating in both tests. Coatings deposited by LPCS show no loss in thickness, regardless of the corrosive environment.

REFERNCES

[1] V.K. Champagne, The cold spray materials deposition process - Fundamentals and applications, 2007 Woodhead Publishing Limited, Cambridge.

[2] A. Papyrin, Cold Spray Technology, 2007 Elsevier, Oxford.

[3] R.G. Maev, V. Leshchynsky, Introduction to Low Pressure Gas Dynamic Spray, 2008 WILEY-VCH Verlag GmbH & Co. KGaA, Weinheim.

[4] H. Katanoda, T. Matsuoka, K. Matsuo, J. Therm. Sci. **16** (1), 40-45 (2006).

[5] B. Jodoin, P. Richer, G. Bérubé, L. Ajdelsztajn, A. Erdi-Betchi, M. Yandouzi, Surf. Coat. Tech. **201**, 7544–7551 (2007).

[6] Xian-Jin Ning, Quan-Sheng Wang, Zhuang Ma, and Hyung-Jun Kim, J. Therm. Spray Tech. **19** (6), 1211-1217 (2010).

[7] T. Schmidt, F. Gärtner, H. Assadi, H. Kreye, Acta Mater. 54, 729–742 (2006).

[8] T. Hussain, D.G. McCartney, P.H. Shipway, D. Zhang, J. Therm. Spray Tech. **18** (3), 364-379 (2009).

[9] V. Luzin, K. Spencer, M.-X. Zhang, Acta Mater. **59**, 1259–1270 (2011).

[10] H. Koivuluoto, J. Lagerbom, M. Kylmalahti, P. Vuoristo, J. Therm. Spray Tech. **17** (5-6), 721-727 (2008).

[11] H. Mäkinen, J. Lagerbom, P. Vuoristo, Thermal Spray 2007: Global Coating Solutions: Proceedings of the 2007 International Thermal Spray Technology, Beijng 2007.

[12] X.-J.Ning, J.-H. Kim, H.-J. Kim, C. Lee, Appl. Surf. Sci. **255**, 3933–3939 (2009).

[13] H. Koivuluoto, P. Vuoristo, J. Therm. Spray Tech. **19** (5), 1081–1092 2010.

[14] Q. Wang, K. Spencer, N. Birbilis, M.-X. Zhang, Surf. Coat. Tech. **205**, 50–56 (2010).

[15] K. Spencer, D.M. Fabijanic, M.-X. Zhang, Surf. Coat. Tech. **204**, 336–344 (2009).

[16] E. Irissou, J.-G. Legoux, B. Arsenault, Ch. Moreau, J. Therm. Spray Tech. **16** (5-6), 661-668 (2007).

[17] H. Koivuluoto and P. Vuoristo, J. Therm. Spray Tech. **18** (4), 555–562 (2009).

[18] Y. Tao, T. Xiong, C. Sun, L. Kong, X. Cui, T. Li, G.-L., Corros Sci **52**, 3191–3197 (2010).

[19] Q. Wang, N. Birbilis, M.-X. Zhang, Mater. Lett. **65**, 1576–1578 (2011).

[20] Davis J. R., Corrosion: Understanding the basics, 2000 ASM International, Materials Park.

[21] Patent no. US 7,736,445 B2, Yagi I., Lu D., Yang X., He D., Surface treatment method for solder join, published 12.11.2008.

[22] Pourbaix M., Atlas of Electrochemical Equilibria in Aqueous Solutions, 1966 National Association of Corrosion, Pergamon.

[23] Lee M. S., Choi H. J., Choi J. W., Kim H. J., Nucl. Eng. Technol. **43**(6), 557-566 (2011).

[24] Ch.G. Munger, L.D. Vincent, Corrosion protection by protective coatings, 1999 National Association of Corrosion Engineers, Houston.

[25] M. G. Fontana, Corrosion engineering, 2005 Tata McGraw-Hill, New York.

[26] R. Baboian, Corrosion tests and standarts, Aplication and interpretation 2nd edition, 2005 ASTM International, Baltimore.

[27] ASTM B117-11, Standard Practice for Operating Salt Spray (Fog) Apparatus, ASTM International, West Conshohocken, PA (2011).

[28] M. Textor, J. Timm, P. Néma, J. Timm, Materialwissenschaft und Werkstofftechnik **26** (6), 318–326 (1995).

[29] J. Song, L. Wang, A. Zibart, C. Koch, Metals **2**, 450-477 (2012).

[30] N.S. Berke, H. E. Townsend, J. Test. Eval. **13** (1), 74-76 (1985).

[31] A. Shkodkin, A. Kashirin, O. Klyuev, and T. Buzdygar, J. of Therm. Spray Tech. **15** (3), 382—386 (2006).

[32] X.-T. Luo, Y.-J. Li, C.-J. Li, Mater. Lett. **163** (15), 58–60 (2016).

[33] S. Kumar G. Bae, K. Kang, S. Yoon, C. Lee, J. Phys. D Appl. Phys. **42**, 075305 (2009).

[34] T. Hong, M. Nagumo, Corros. Sci. **39** (9), 1665–1672 (1997).

[35] A. Shahryari, W. Kamal, S. Omanovic, Mater. Lett. **62** (23), 3906–3909 (2008).

[36] H.-R. Wang, B.-R. Hou, J. Wang, Q. Wang, W.-Y. Li, J. Therm. Spray Tech. **17** (5-6), 736–741 (2008).

[37] J. Baszkiewicz, M. Kamiński, Korozja materiałów, 2006 Oficyna Wydawnicza Politechniki Warszawskiej, Warszawa.

[38] M. Schutze, Corrosion and environmental degradation. Vol. 2, 2000 Wiley-VCH, Weinheim.

[39] E. Otero, J.M. Bastidas, W. Lopez, J.L.G. Fierro, Werkstoffe und Korrosion **45**, 387-393 (1994).

[40] J.R. Davis, Handbook of thermal spray technology, 2004 ASM International, Materials Park4.